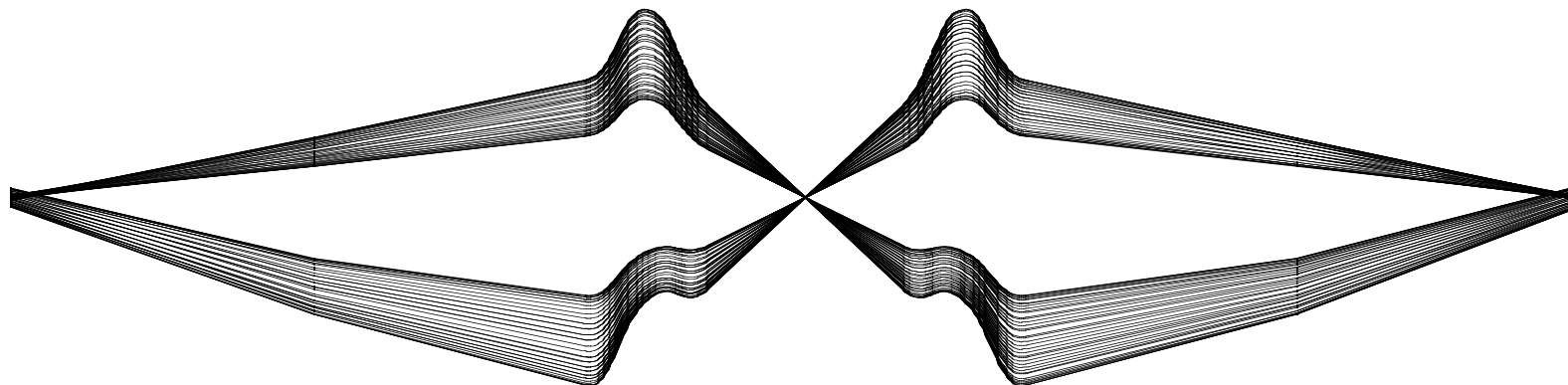


THE RAY-TRACING CODE ZGOUBI



**F. Méot
CEA & IN2P3, LPSC
Grenoble**

Contents

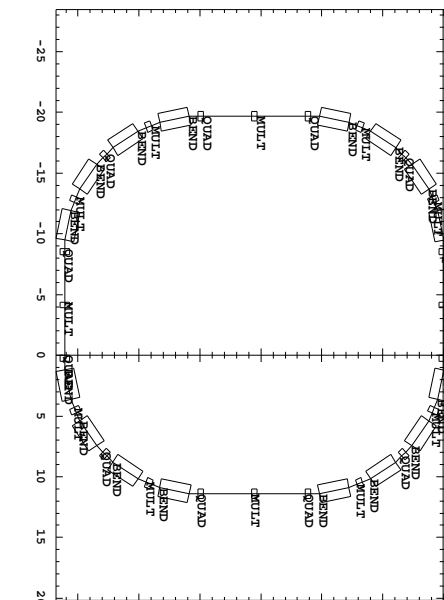
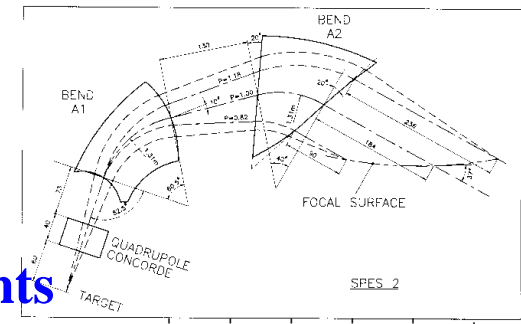
1	Introduction	3
1.1	What Zgoubi can do	3
1.2	The numerical integration method	5
2	Tracking FFAGs	8
2.1	Radial scaling triplet using ``FFAG'', 6-D tracking simulations	12
2.2	Radial triplet represented by 3-D field maps, using ``TOSCA''	16
2.3	``FFAG-SPI'', 17→180 MeV acceleration in RACCAM	19
2.4	NuFact linear FFAG using ``MULTIPOL'', 6-D transmission	20
2.5	EMMA	22
2.5.1	EMMA using ``MULTIPOLE'', full acceleration cycle	22
2.5.2	Closer to actual field shape : EMMA using ``DIPOLES''	25
2.5.3	The idea, more precisely :	26
2.5.4	A new procedure for field maps, ``EMMA''	27
2.6	Pumplet-cell I-FFAG using ``DIPOLES'', full acceleration cycle	29
3	Synchrotron radiation	31
4	Spin	35

1 Introduction

1.1 What Zgoubi can do

Calculate trajectories of charged particles in magnetic and electric fields.

- At the origin (early 1970's) developped for design and operation of
 - beam lines
 - magnetic spectrometers
- Zgoubi has so evolved that it allows today the study of
 - systems including complex sequences of optical elements
 - periodic structures
- and allows accounting for additional properties as
 - synchrotron radiation and its dynamical effects
 - spin tracking
 - in-flight decay
 - etc...
 - FAQ : *not space charge (not yet ?)*



it provides numerous Monte Carlo methods

- **object definition**
- **stochastic SR**
- **in-flight decay**
- **etc.**

- **a built-in fitting procedure including**
 - arbitrary variables
 - * any data in the input file can be varied
 - a large variety of constraints,
 - * easily extendable to even more

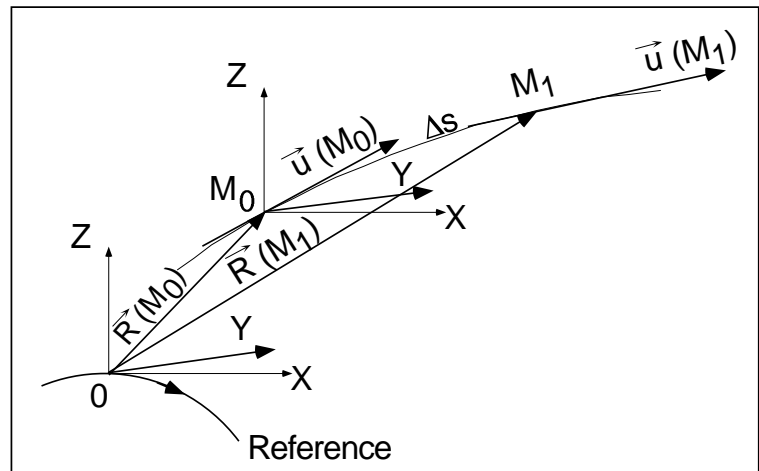
- **multiturn tracking in circular accelerators including**
 - features proper to machine parameter calculation and survey,
 - simulation of time-varying power supplies,
 - * any element individually (allows tune-jump, etc.)
 - etc.

1.2 The numerical integration method

MOTION, from M_0 to M_1

The equation of motion

$$d(m\vec{v}) = q(\vec{e} + \vec{v} \times \vec{b}) dt$$



- is solved using truncated Taylor expansions of \vec{R} and $\vec{u} = \vec{v}/v$:

$$\begin{aligned}\vec{R}(M_1) &\approx \vec{R}(M_0) + \vec{u}(M_0) \Delta s + \vec{u}'(M_0) \frac{\Delta s^2}{2!} + \dots + \vec{u}''''''(M_0) \frac{\Delta s^6}{6!} \\ \vec{u}(M_1) &\approx \vec{u}(M_0) + \vec{u}(M_0) \Delta s + \vec{u}''(M_0) \frac{\Delta s^2}{2!} + \dots + \vec{u}''''''(M_0) \frac{\Delta s^5}{5!}\end{aligned}\quad (1)$$

- In non-zero \vec{E} environment, rigidity at M_1 is re-computed :

$$(B\rho)(M_1) \approx (B\rho)(M_0) + (B\rho)'(M_0) \Delta s + \dots + (B\rho)''''(M_0) \frac{\Delta s^4}{4!} \quad (2)$$

- When necessary, time-of-flight is computed in a similar manner :

$$T(M_1) \approx T(M_0) + \frac{dT}{ds}(M_0) \Delta s + \frac{d^2T}{ds^2}(M_0) \frac{\Delta s^2}{2} + \frac{d^3T}{ds^3}(M_0) \frac{\Delta s^3}{3!} + \frac{d^4T}{ds^4}(M_0) \frac{\Delta s^4}{4!} \quad (3)$$

- In a general manner, the truncated Taylor series

$$\begin{aligned}
 \vec{R}(M_1) &= \vec{R}(M_0) + \vec{u}(M_0) \Delta s + \dots \\
 \vec{u}(M_1) &= \vec{u}(M_0) + \vec{u}'(M_0) \Delta s + \dots \\
 (B\rho)(M_1) &= (B\rho)(M_0) + (B\rho)'(M_0) \Delta s + \dots \\
 T(M_1) &= T(M_0) + \frac{dT}{ds}(M_0) \Delta s + \dots
 \end{aligned} \tag{4}$$

require computation of the derivatives

$$\vec{u}^{(n)} = d^n \vec{u} / ds^n$$

$$(B\rho)^{(n)} = d^n (B\rho) / ds^n$$

$$d^n(T) / ds^n$$

Integration in magnetic fields

- Let's introduce simplified notations :

$$\vec{u} = \frac{\vec{v}}{v}, \quad ds = v dt, \quad \vec{u}' = \frac{d\vec{u}}{ds}, \quad m\vec{v} = mv\vec{u} = q B\rho \vec{u} \quad \vec{B} = \frac{\vec{b}}{B\rho} \quad (5)$$

$d(m\vec{v}) = q (\vec{e} + \vec{v} \times \vec{b}) dt$ (with $\vec{e} = 0$) then writes

$$\boxed{\vec{u}' = \vec{u} \times \vec{B}}$$

This yields the $\vec{u}^{(n)} = d^n \vec{u} / ds^n$ needed in the Taylor expansions : $\vec{u}' = \vec{u} \times \vec{B}$

$$\begin{aligned} \vec{u}'' &= \vec{u}' \times \vec{B} + \vec{u} \times \vec{B}' \\ \vec{u}''' &= \vec{u}'' \times \vec{B} + 2\vec{u}' \times \vec{B}' + \vec{u} \times \vec{B}'' \\ \vec{u}'''' &= \vec{u}''' \times \vec{B} + 3\vec{u}'' \times \vec{B}' + 3\vec{u}' \times \vec{B}'' + \vec{u} \times \vec{B}''' \\ \vec{u}''''' &= \vec{u}'''' \times \vec{B} + 4\vec{u}''' \times \vec{B}' + 6\vec{u}'' \times \vec{B}'' + 4\vec{u}' \times \vec{B}''' + \vec{u} \times \vec{B}''''' \end{aligned} \quad (6)$$

where $\vec{B}^{(n)} = d^n \vec{B} / ds^n$.

2 Tracking FFAGs

- Accelerator R&D domains concerned :
 - NuFact
 - scaling lattice
 - linear non-scaling lattice
 - EMMA
 - Medical
 - scaling lattice
 - linear non-scaling lattice
 - quasi-linear non-scaling lattice
 - p-driver
 - scaling lattice
 - linear non-scaling lattice
 - quasi-linear non-scaling lattice
 - pumplet lattice
 - etc.
 - In all cases : 2-D and 3-D field map based ray-tracing

- Optics :

- Scaling FFAG simulations need special elements, like

- [sector, spiral,...] dipoles with “arbitrary” axial (including fringe field effects) and radial dependence of magnetic field

$$B_{zi}(r, \theta) = B_{z0,i} \mathcal{F}_i(r, \theta) \mathcal{R}_i(r)$$

- Scaling FFAG, NC magnets (“FFAG” procedure) :

$$\mathcal{R}_i(r) = (r/R_{0,i})^{K_i}$$



- Scaling FFAG, SC magnets (“Dipoles” procedure) :

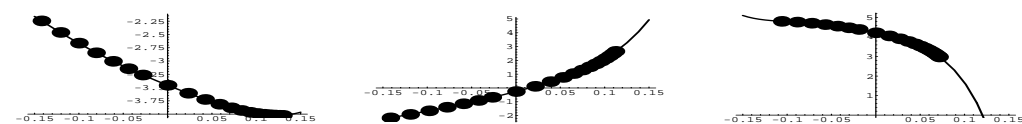
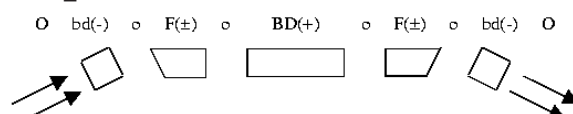
$$\mathcal{R}_i(r) = b_{0i} + b_{1i}(r - R_{0,i})/R_{0,i} + b_{2i}(r - R_{0,i})^2/R_{0,i}^2 + \dots$$



- accounting for possible variable gap $g = g_0(R_0/r)^K$,
and overlapping of fringe fields

- Linear FFAGs are built from quadrupole fields, the “MULTIPOLE” procedure in Zgoubi is employed to simulate that. These FFAGs did not necessitate any particular development.

- The isochronous type of FFAG lattice (“pumplet”) is simulated combining “MULTIPOLE” and “Dipoles” procedures.



- **RF :** not a real issue up to now :
- Regular point transforms seems to answer FAQs
- The question of TOF in terms of a reference particle, or absolute TOF computation sometimes arise - well managed by the ray-tracing methods up to now
- **This has been confirmed experimentally :**
acceleration is achieved successfully in a number of different RF regimes (detailed simulations published, see FFAG workshop series) :
 - RF swing in radial S-FFAG lattice (cf. KEK 150 MeV)
 - RF swing in spiral S-FFAG lattice (cf. RACCAM)
 - RF swing in linear NS-FFAG lattice (cf. PAMELA by T. Yokoi et al.)
 - fixed, low RF frequency, stationary bucket mode, in S-FFAG (cf. PRISM ; muon accelerators in NuFact)
 - fixed, high RF frequency, serpentine mode, in NS-FFAG (cf. EMMA ; muon accelerators in NuFact)
 - fixed, high RF frequency, quasi-isochronous mode, in semi-NS-FFAG (“Pumplet” lattice)
- **More realistic, pill-box or other type of cavities** will be introduced for NuFact R&D,
- **as well as 4-D electromagnetic field maps**

• Automatic matching

An indispensable tool for

- preliminary adjustments (tunes, etc.) prior to 6-D simulations
- considered very useful for further assessment and optimisation of higher order behavior, DA, transmission, ...

FIT CONSTRAINTS :

Trajectory coordinates (e.g., final coordinates)

Several other types of quantities that are deduced from trajectories, e.g. :

- first and higher order transport coefficients
- beam matrix coefficients (waist, divergence)
- particle fluxes through ellipses (→ transmission efficiency)

In the case of periodic structures :

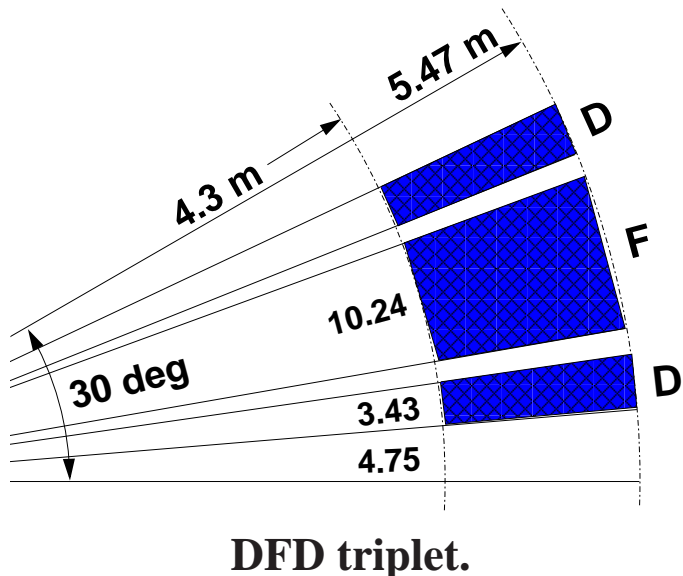
- closed orbits
- tunes, chromaticites, anharmonicities

FIT VARIABLES, WHICH ? ANY !

```
'OBJET' * c.o., constant Gap *
226.8235847      68MeV/c muon
2
2 1
499.377   0.   0.   0.   0.   1.2   'b'
1 1 1 1 1 1 1 1
'FFAG'
0
3 45.   500.                               NMAG, Sector angle R0
18.17  0.  -0.717  5.                      mag 1 : ACNT, dum, B0, K
6.3  0.                                     EFB 1 : lambda, gap, const/v
4 .1455  2.2670  -.6395  1.1558  0.  0.  0.
1.23 0.  1.E6  -1.E6  1.E6  1.E6
6.3 0.                                     EFB 2
4 .1455  2.2670  -.6395  1.1558  0.  0.  0.
-1.23 0.  1.E6  -1.E6  1.E6  1.E6
0. -1                                     EFB 3 : inhibited by iop=0
0 0.   0.   0.   0.   0.   0.   0.
0. 0.   0.   0.   0.   0.   0.   0.
22.5 0.  3.2  5.                           mag 2 : ACNT, B0, K, dums
6.3 0.                                     EFB 1
4 .1455  2.2670  -.6395  1.1558  0.  0.  0.
3. 0.  1.E6  -1.E6  1.E6  1.E6
6.3 0.                                     EFB 2
4 .1455  2.2670  -.6395  1.1558  0.  0.  0.
-3 0.  1.E6  -1.E6  1.E6  1.E6
0. -1                                     EFB 3
0 0.   0.   0.   0.   0.   0.   0.
0. 0.   0.   0.   0.   0.   0.   0.
26.83 0.  -0.717  5.                      mag 3 : ACNT, dum, B0, K
6.3 0.                                     EFB 1
4 .1455  2.2670  -.6395  1.1558  0.  0.  0.
1.23 0.  1.E6  -1.E6  1.E6  1.E6
6.3 0.                                     EFB 2
4 .1455  2.2670  -.6395  1.1558  0.  0.  0.
-1.23 0.  1.E6  -1.E6  1.E6  1.E6
0. -1                                     EFB 3
0 0.   0.   0.   0.   0.   0.   0.
0. 0.   0.   0.   0.   0.   0.   0.
0   2 125.                                KIRD anal/num, resol(mesh=step/resol)
.5
2 0.   0.   0.   0.   0.
```

2.1 Radial scaling triplet using ‘‘FFAG’’, 6-D tracking simulations

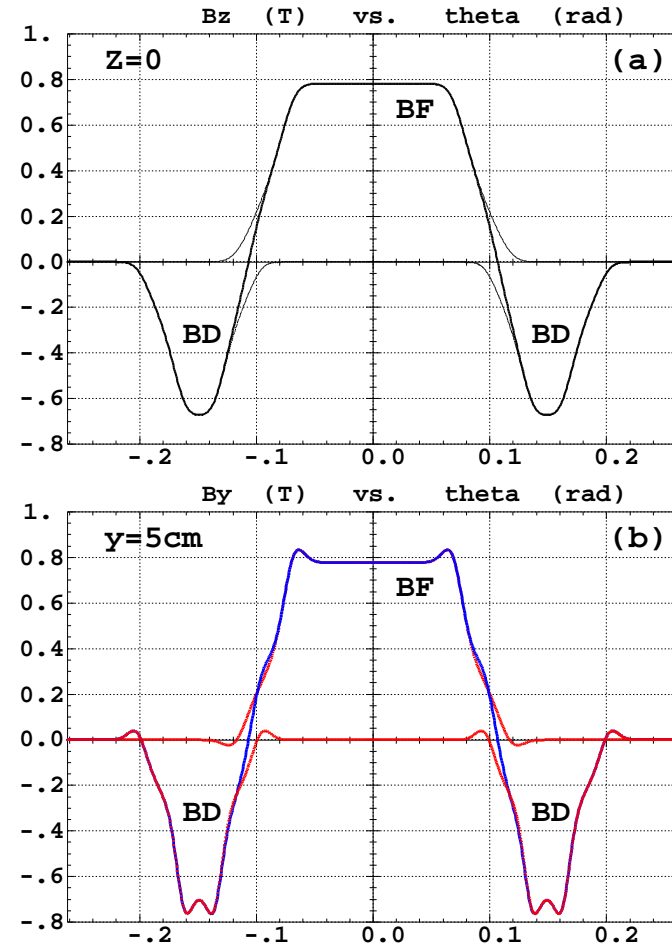
The “FFAG” procedures is used to simulate $B_{zi}(r, \theta) = B_{z0,i} \mathcal{F}_i(r, \theta) \mathcal{R}_i(r)$ AND allow overlapping of fringe fields in a scaling FFAG triplet :



The geometrical model is based on the superposition of the independent contributions of the N dipoles :

$$B_z(r, \theta) = \sum_{i=1,N} B_{z0,i} \mathcal{F}_i(r, \theta) \mathcal{R}_i(r)$$

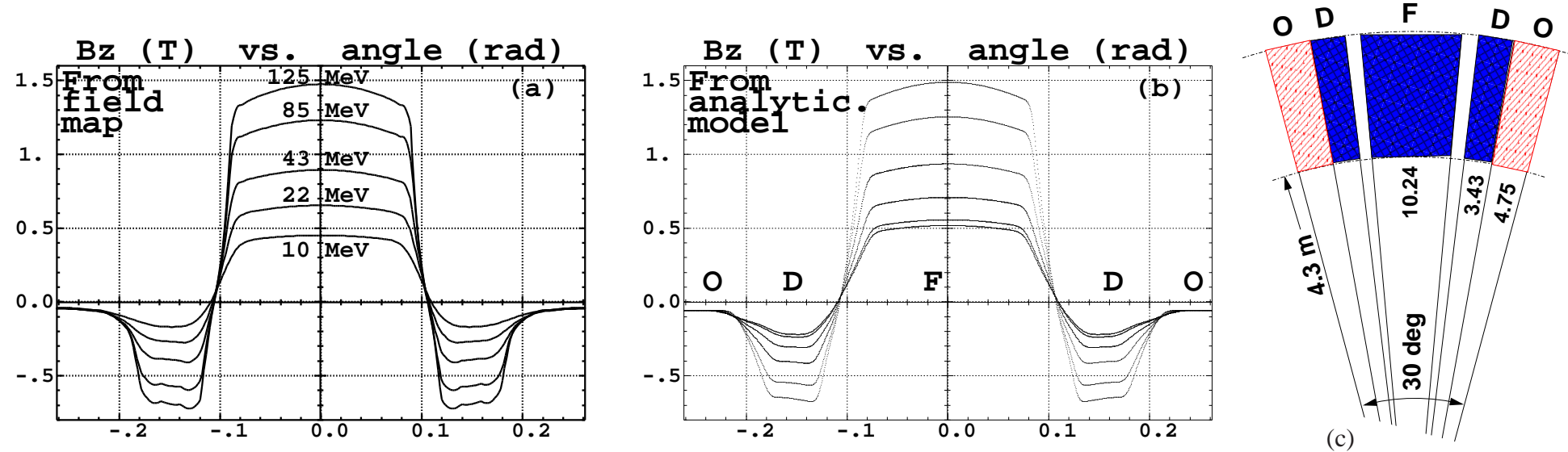
at all (r, θ) in the mid-plane. Field off mid-plane is obtained by Taylor expansion.



Field experienced for $r_0 = 4.87$ m in the DFD dipole triplet.
A superposition of $N = 3$ independent contributions, at all (r, θ, z) .

- It has been tested by simulating the KEK 150 MeV FFAG [Details in : NIM A 547 (2005)]

2 more dipoles are introduced to create the continuous ~ 700 Gauss stray field in te drift.



Comparison of magnetic field along closed orbits in the case of,

(a) : TOSCA 3-D map representative of the 150 MeV FFAG, and,

(b) : field from the “3+2”-dipole geometrical model.

(c) shows the geometry of the “3+2”-dipole design, including two additional dipole regions (hatched) that simulate 700 G field extent over the two end drifts.

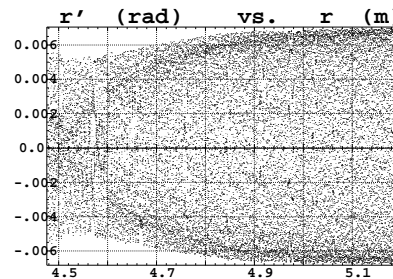
- A particle with $z_0 = 3 \text{ cm}$ (a large value !) accelerated from 12 to 125 MeV.

A/ Case of analytical calculation of field derivatives (the Zgoubi method needs the $d^n B/ds^n$)

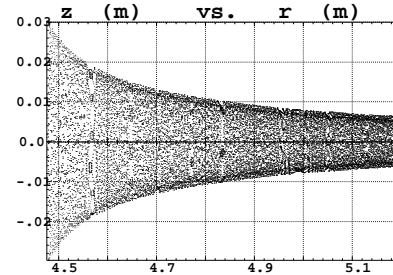
Method : $d^n B/ds^n$ computed from the geometrical model of the (r, θ) field dependence, and from distances to EFBs.

Interest : accurate (good for symplecticity), fast (larger step size).

x-z coupling, yet $\epsilon_x \approx 0$



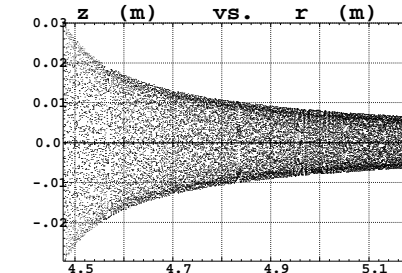
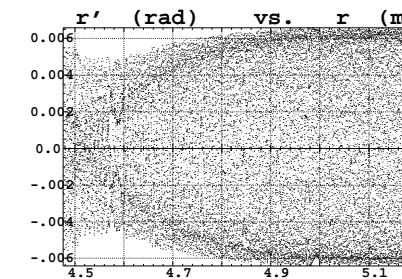
ϵ_z -damping $\propto \sqrt{\beta\gamma}$



B/ Case of numerical calculation of field derivatives

Method : $d^n B/ds^n$ computed from numerical interpolation between small set of field values surrounding the particle.

Interest : allows easier implementation/exploration of complex types of (r, θ) field dependences.

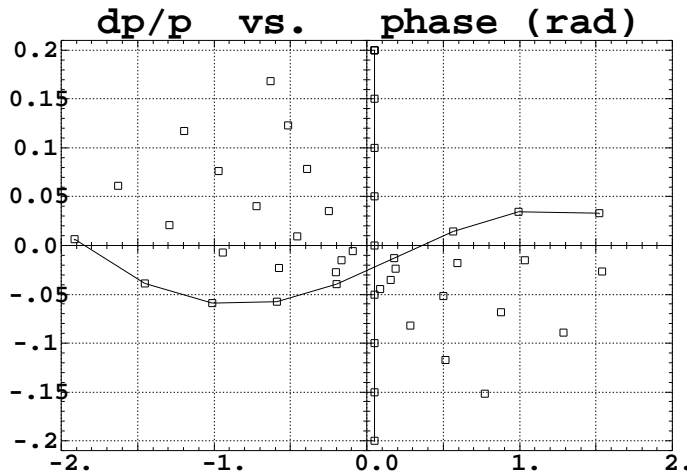


A large step size is used, in both cases : 0.5 cm, with success.

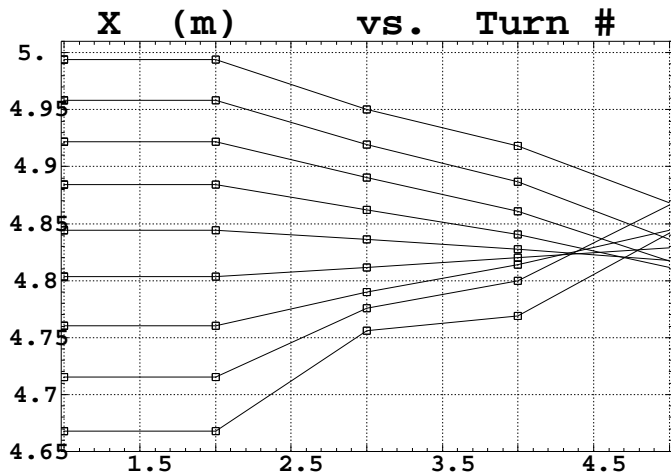
This is allowed thanks to the accuracy of the integration method.

- A rough test of stationary bucket type of acceleration : PRISM

Bunch rotation in 5 turns (a simplistic
RF wave is used, sine-like) :



Radial compression :



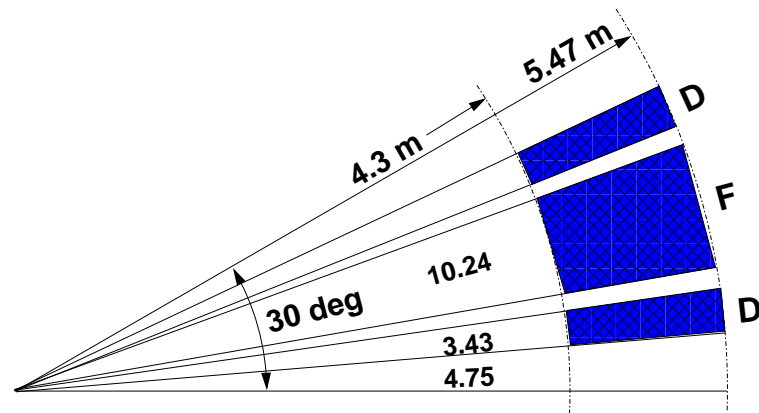
Data file - 45deg. period (drift-DFD-drift) :

```
'OBJET' * c.o., constant Gap *
226.8235847      68MeV/c muon
2
2 1
499.377  0.  0.  0.  0.  1.2  'b'
1 1 1 1 1 1 1 1
'FFAG'
0
3 45.      500.
18.17  0.  -0.717  5.
6.3  0.
4 .1455   2.2670  -.6395  1.1558  0.  0.  0.
1.23 0.    1.E6   -1.E6  1.E6  1.E6
6.3  0.
4 .1455   2.2670  -.6395  1.1558  0.  0.  0.
-1.23 0.   1.E6   -1.E6  1.E6  1.E6
0. -1
0 0.      0.  0.  0.  0.  0.  0.
0. 0.      0.  0.  0.  0.  0.  0.
22.5 0.    3.2  5.
6.3  0.
EFB 1
4 .1455   2.2670  -.6395  1.1558  0.  0.  0.
3.  0.    1.E6   -1.E6  1.E6  1.E6
6.3  0.
EFB 2
4 .1455   2.2670  -.6395  1.1558  0.  0.  0.
-3  0.   1.E6   -1.E6  1.E6  1.E6
0. -1
EFB 3
0 0.      0.  0.  0.  0.  0.  0.
0. 0.      0.  0.  0.  0.  0.  0.
mag 2 : ACNT0.3927rad, m, B0, K,dummie
EFB 1
4 .1455   2.2670  -.6395  1.1558  0.  0.  0.
3.  0.    1.E6   -1.E6  1.E6  1.E6
6.3  0.
EFB 2
4 .1455   2.2670  -.6395  1.1558  0.  0.  0.
-3  0.   1.E6   -1.E6  1.E6  1.E6
0. -1
EFB 3
0 0.      0.  0.  0.  0.  0.  0.
0. 0.      0.  0.  0.  0.  0.  0.
mag 3 : ACNT, dum, B0, K
EFB 1
26.83 0.  -0.717  5.
6.3  0.
EFB 2
4 .1455   2.2670  -.6395  1.1558  0.  0.  0.
1.23 0.   1.E6   -1.E6  1.E6  1.E6
6.3  0.
EFB 3
4 .1455   2.2670  -.6395  1.1558  0.  0.  0.
-1.23 0.  1.E6   -1.E6  1.E6  1.E6
0. -1
EFB 3
0 0.      0.  0.  0.  0.  0.  0.
0. 0.      0.  0.  0.  0.  0.  0.
0 2 125.
.5
2 0.  0.  0.  0.  0.
```

KIRD anal/num (=0/2,25,4), resol(mesh=st integration step size (cm))

2.2 Radial triplet represented by 3-D field maps, using "TOSCA"

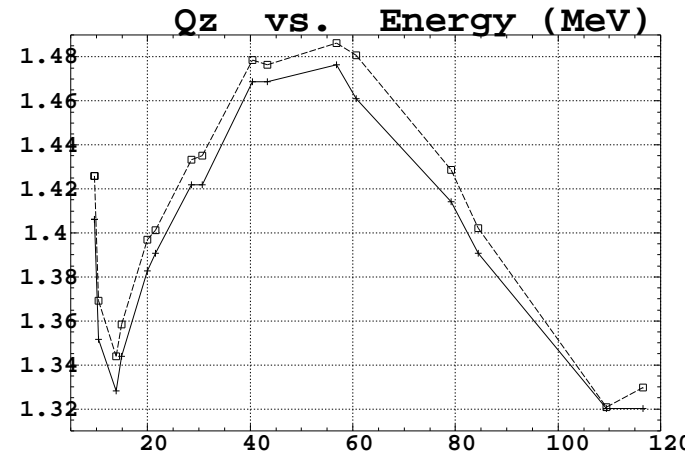
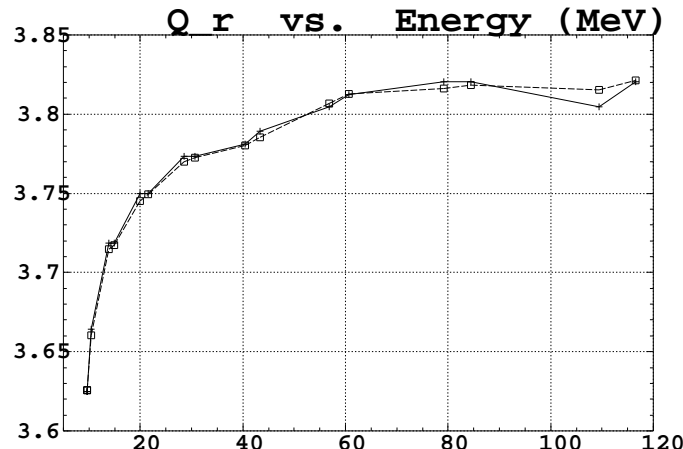
[Details in : CERN NuFact Note 140 (2004)]



Geometry of the DFD sector triplet and 30 degrees sector cell.



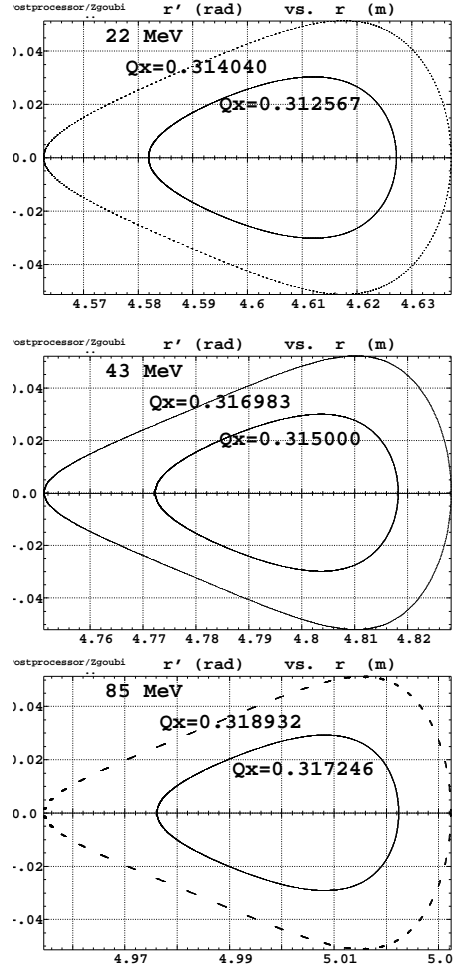
Geometry of TOSCA field map, covering half the angular extent.



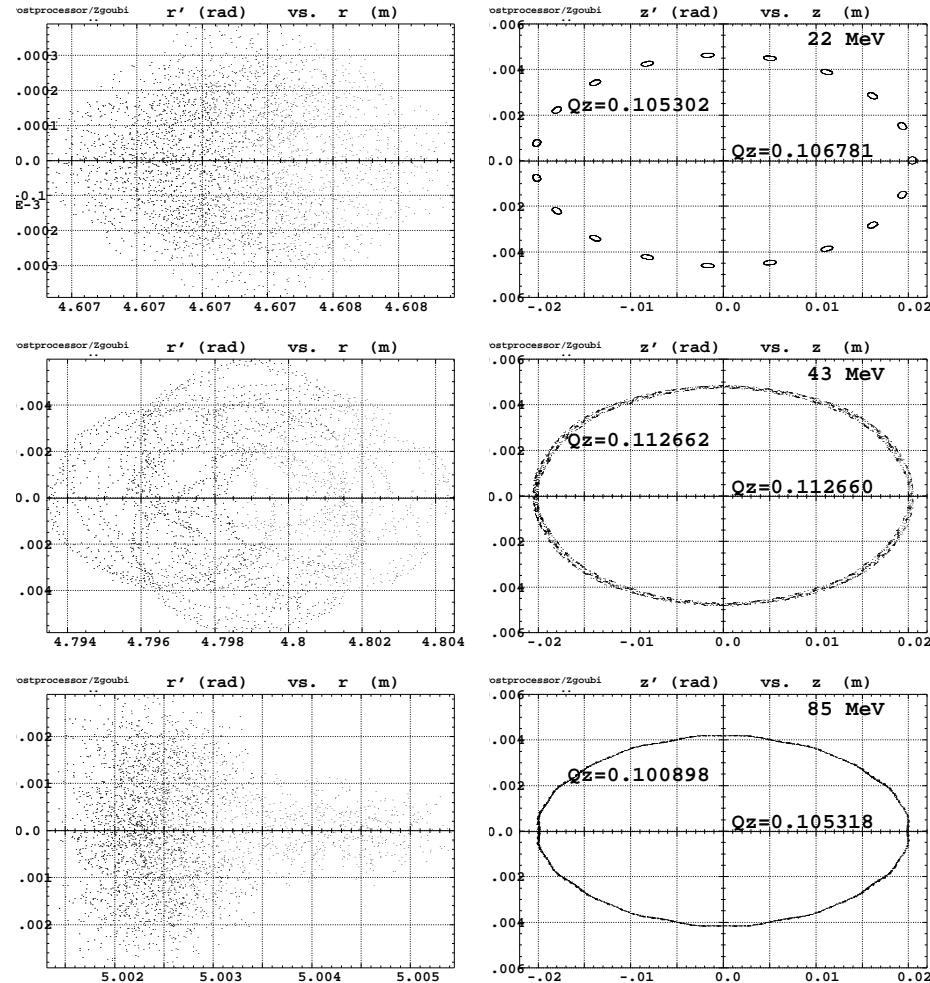
Radial tune (left plot) and axial tune (right) as a function of energy, as obtained using RK4 integration (solid lines/crosses), or using Zgoubi (dashed line/squares).

The results below make clear that the symplecticity is very good (“precision to order Δs^6 ”) even when using field maps.

Note that, the mesh size needs be very small, \approx mm, and the integration step size must stick.

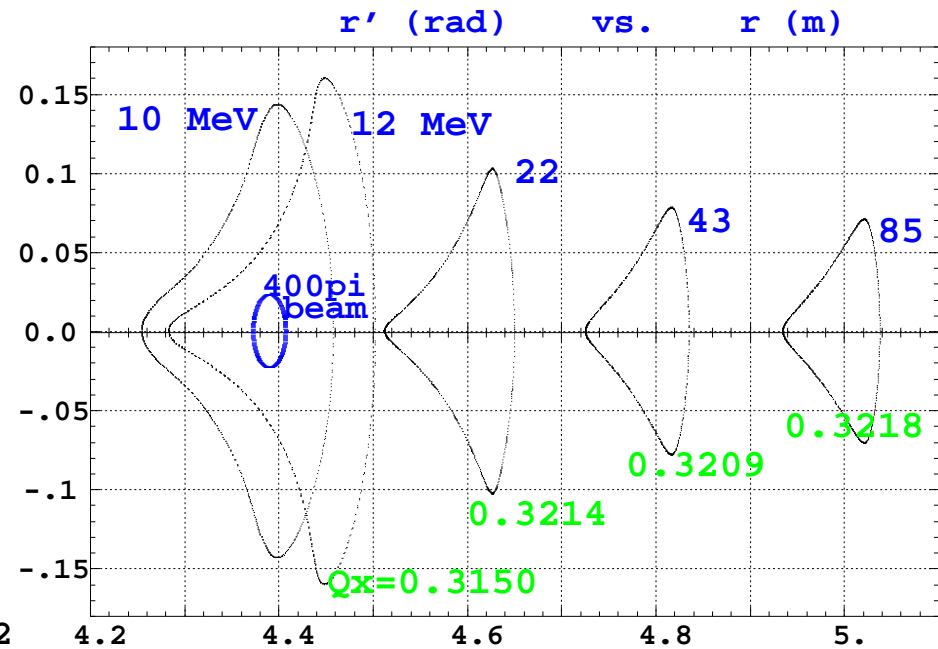
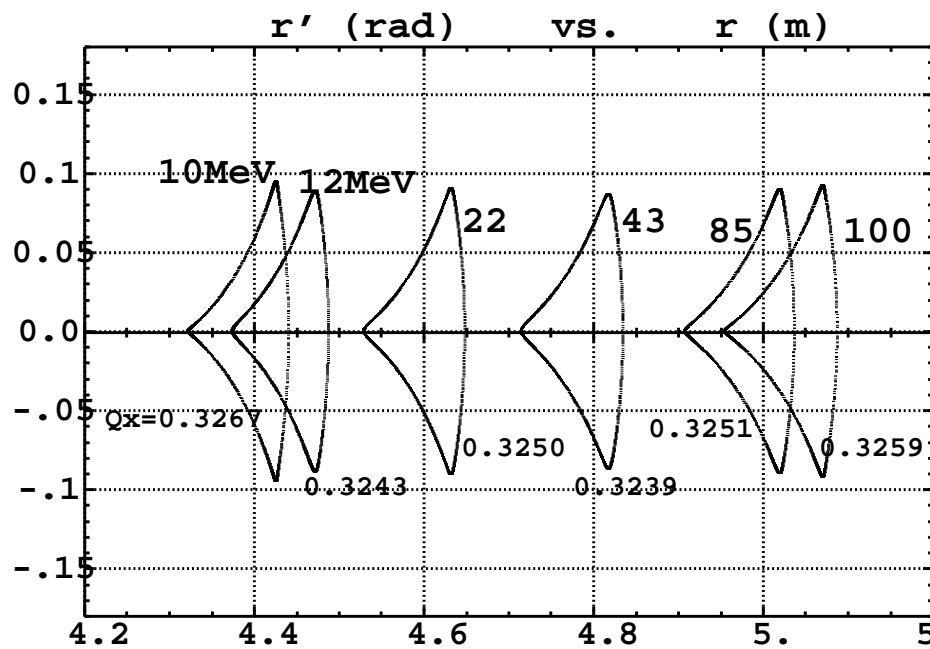


Horizontal motion, near stability limit.
The inner motion is 3500 pass in a cell
the outer one is 4700.



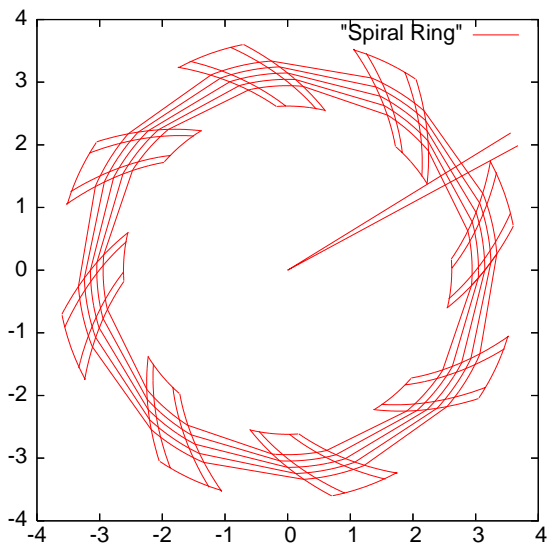
Right column : vertical phase-space for $z_0 = 2$ cm with $r_0 = r_{closed\ orbit}$.
Left column : corresponding horizontal motion. 3200 periods.

- Comparison between “FFAG” procedure and 3-D field maps

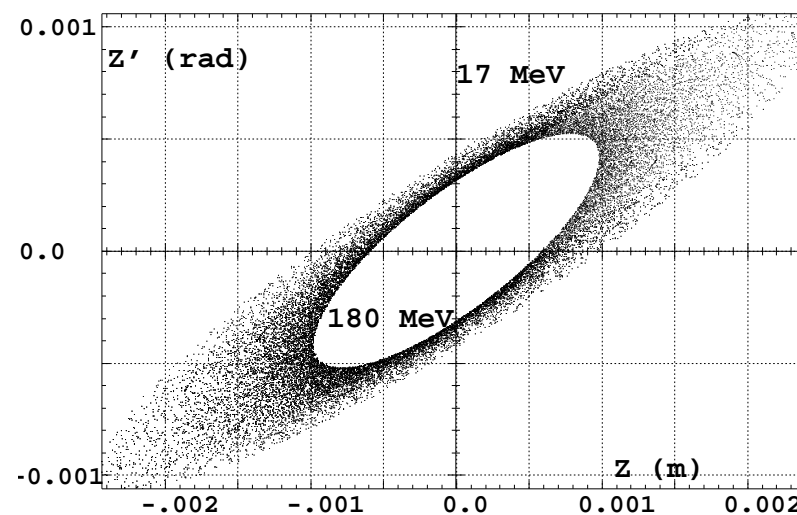


150MeV FFAG : horizontal phase space, the limits of stable motion, for 5 energies.
For comparison : tracking with geometrical model (left), or using TOSCA map (right).

2.3 ``FFAG-SPI'', 17→180 MeV acceleration in RACCAM



A scheme of RACCAM spiral ring and a set of closed orbits taken between 0.6 T.m (17 MeV proton) and 2 T.m (180 MeV).



Adiabatic damping of vertical motion over an acceleration cycle, 50000 turns.

The RF phase $\phi(t) = 2\pi \int_0^t f_{RF}(t)dt$ upon arrival of a particle at the RF gap at time t , is computed by interpolating f_{RF} from the inverse of the revolution time

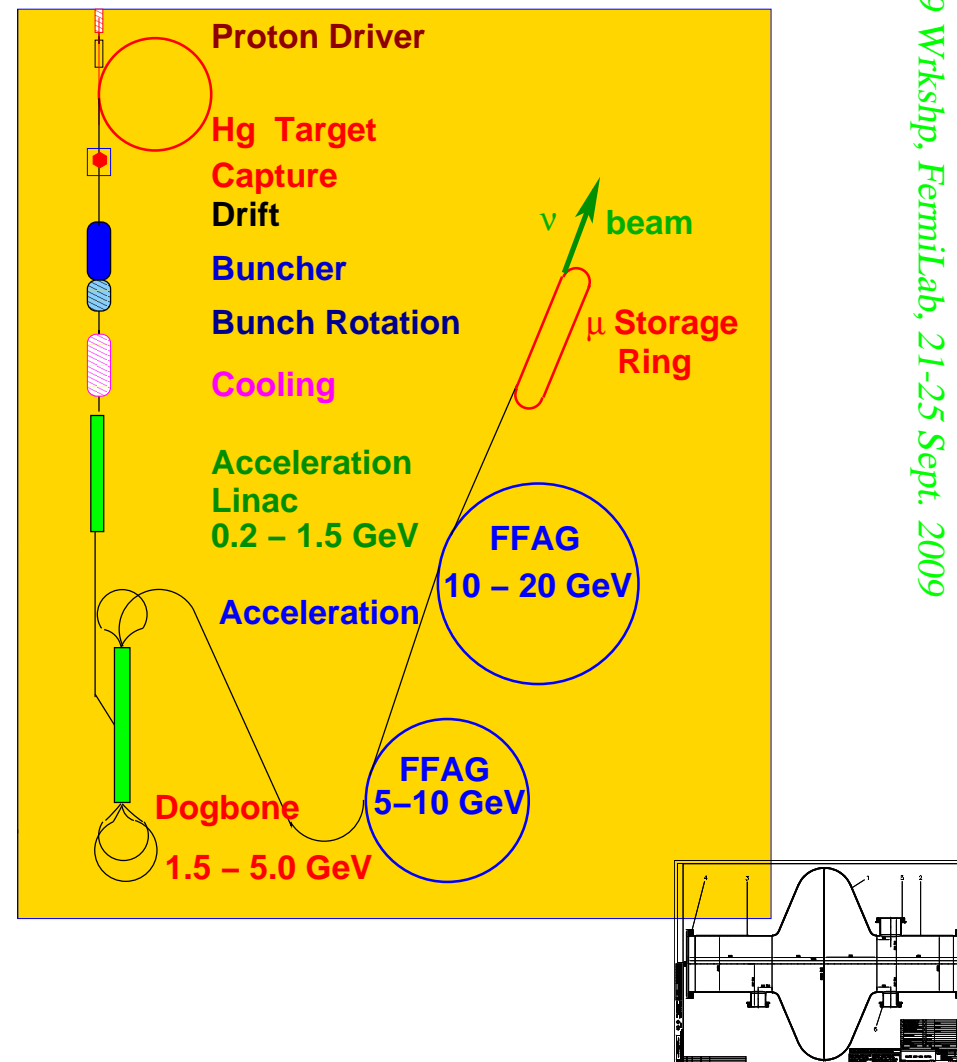
$$\tau = \tau_0 \left(\frac{p}{p_0} \right)^{\frac{-k}{k+1}} \frac{E}{E_0}$$

2.4 NuFact linear FFAG using ``MULTIPOL'', 6-D transmission

Lattice parameters

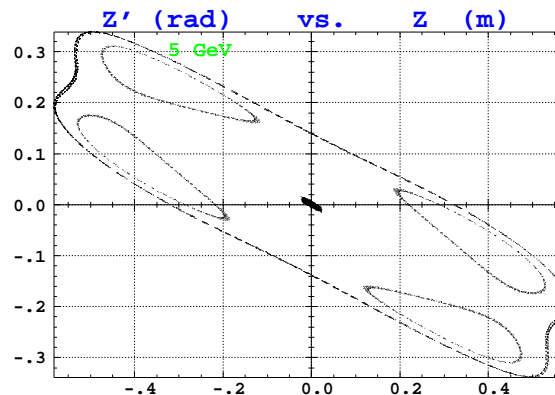
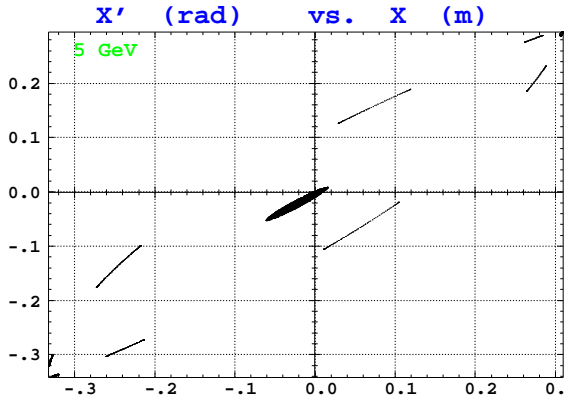
ISS data :

Energy	(GeV)	2.5→5	5→10	10→20
No. of cells		52	64	84
No. of turns		4.8	9	15.5
Circumference	(m)	210	285	410
D magnet :				
length	(m)	0.6	0.75	0.93
radius	(cm)	13.2	9.8	7.5
pole tip field	(T)	4.7	6.1	7.5
F magnet :				
length	(m)	0.95	1.20	1.45
radius	(cm)	20.7	16.6	13.3
pole tip field	(T)	2.7	3.4	4.2
No. of cavities		42	(46)	54
Zgoubi :				
E gain/cav.	(MeV)	12.5	12.4	12.7



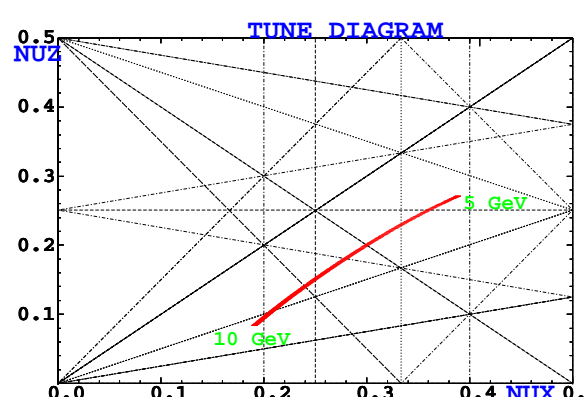
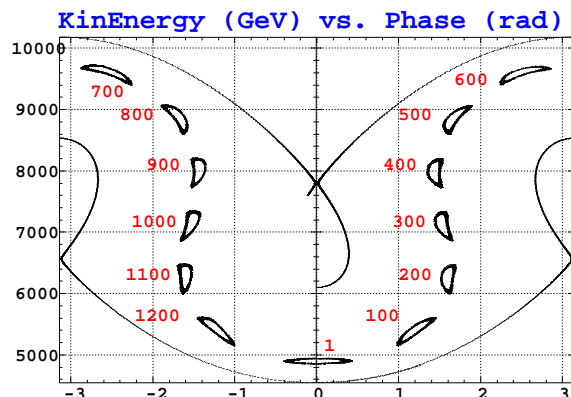
- F/D quadrupole doublet \Rightarrow "MULTIPOLE"
- Acceleration : one cavity every cell. $\hat{V} = 9.928$, Rf freq. 202.332 MHz.

Injected beam ($> 3\pi \text{cm}/0.05 \text{ eV.s}$) is well within stability limits



Phase-Energy motion,

Beam path in tune diagram



2.5 EMMA

2.5.1 EMMA using ‘‘MULTIPOLE’’, full acceleration cycle

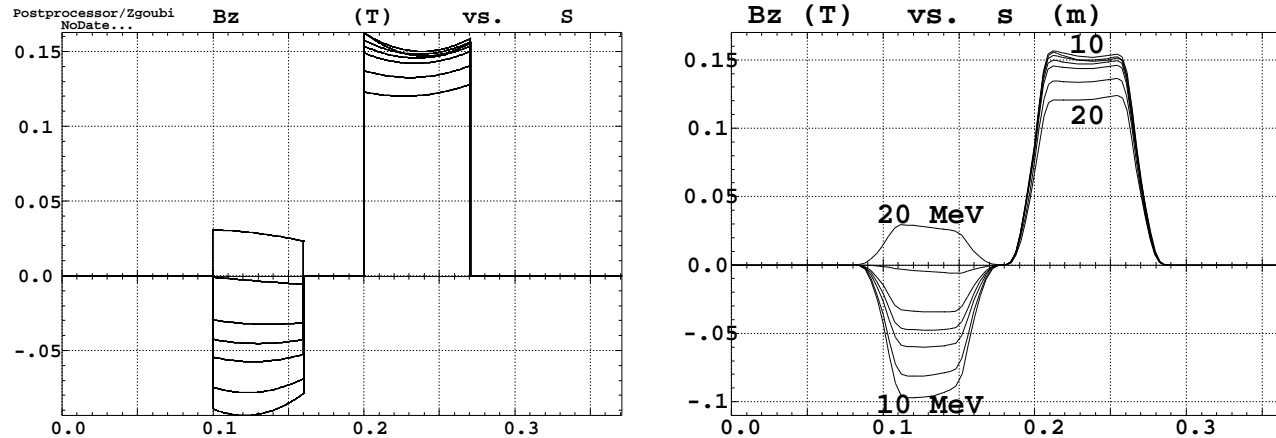


Figure 1: Field on closed orbits at various energies, without (left) and with (right) fringe fields.

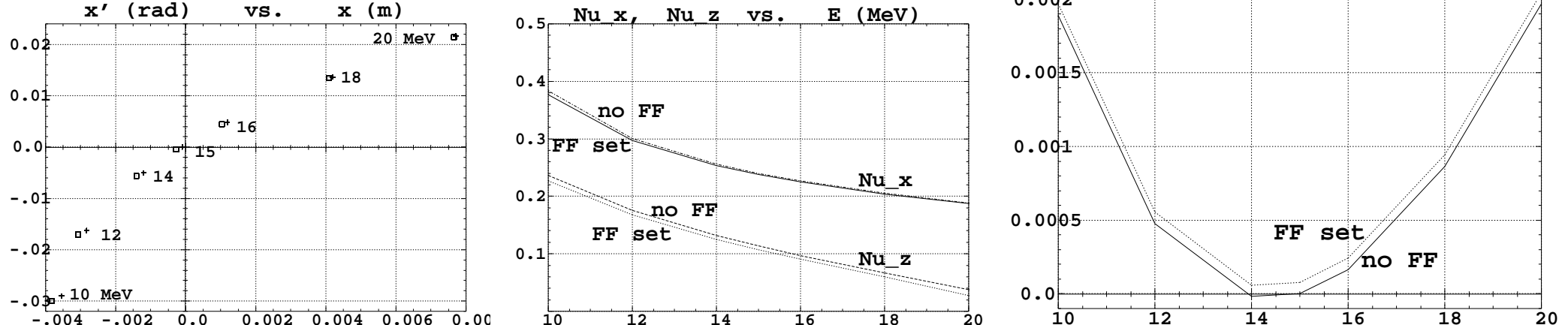


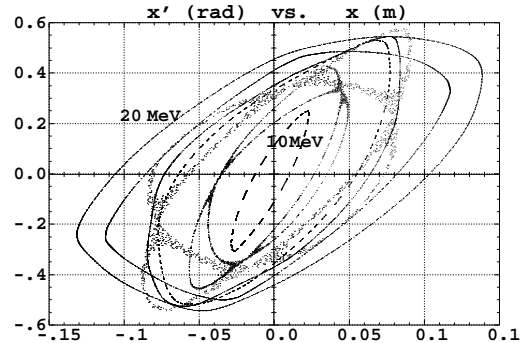
Figure 2: Left : energy dependence of the horizontal closed orbits in (x, x') phase space, with (squares) or without (crosses) fringe fields.

Middle : Tunes as a function of energy. Right : $(T - T_{Ref})/T_{Ref}$ as a function of energy.

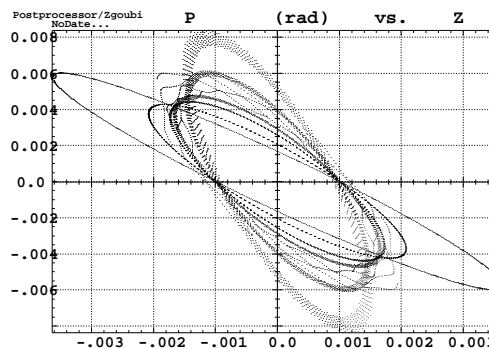
Stability limits

2000-cell H stability limits, about 5% precision in x ,
at 10, 12, 14, 15, 16, 18 and 20 MeV.

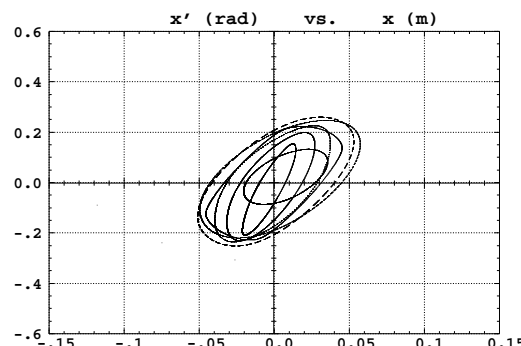
Pure horizontal motion, no fringe fields :



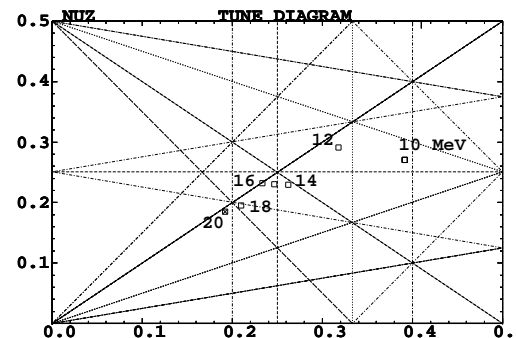
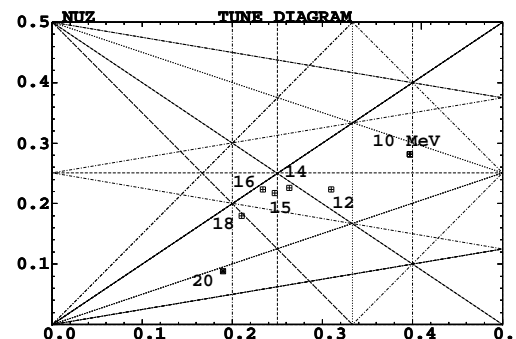
Vertical motion in the $\approx 200 \pi$ (norm.) region :



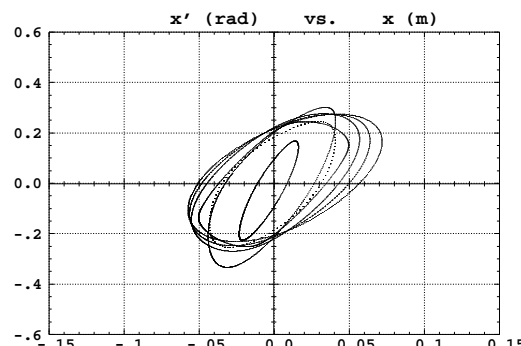
In presence of very small z motion, no fringe fields :



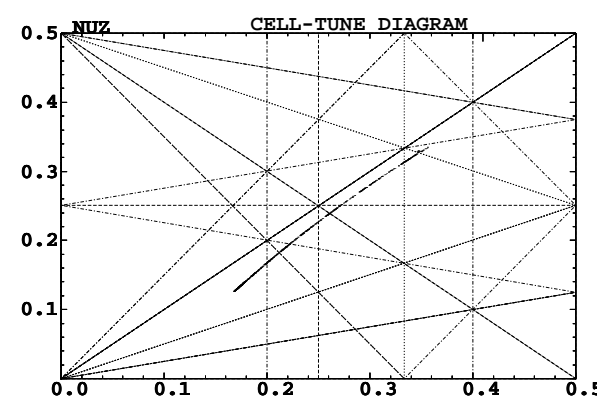
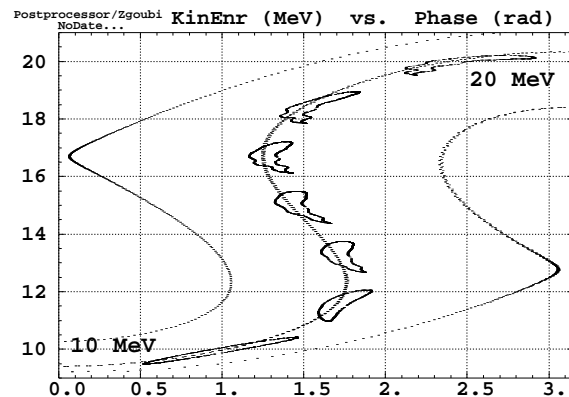
Cell tunes at stability limits (resonance lines up to 5th order are represented) :



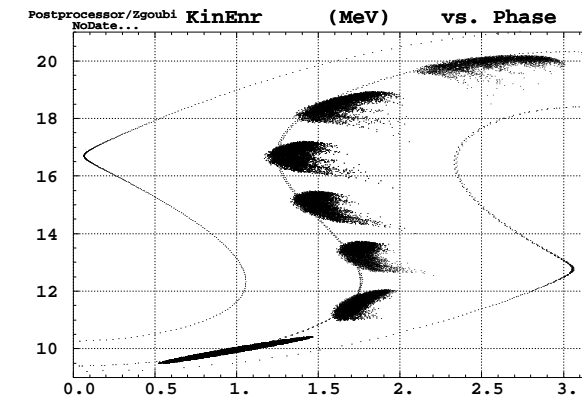
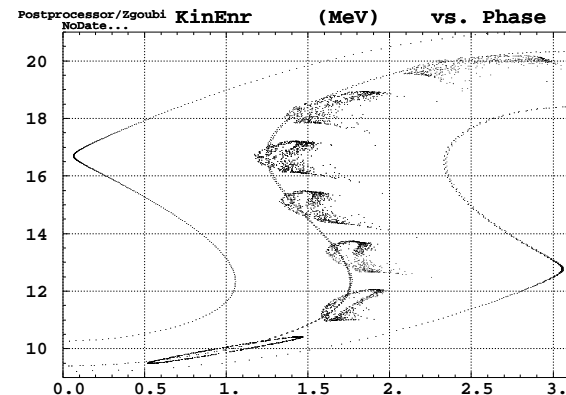
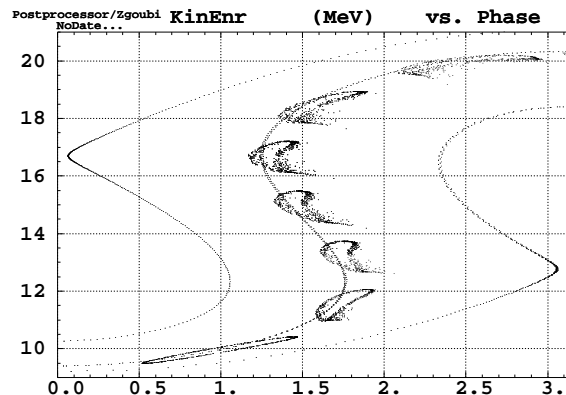
In presence of very small z motion, fringe fields set :



Longitudinal serpentine motion



- Acceleration of 1000 electrons on an ellipse, zero transverse emittances, from 10 to 20 MeV in 125 cavity passes.
 - Three particular trajectories show the separatrix and the bunch cog.
 - Voltage : 70 kV peak, RF freq. : 1.3552 GHz.

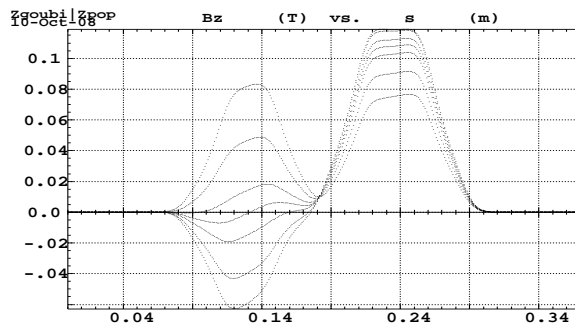


- The sensible effect of launching a bunch with non-zero transverse size.
- Left : $\epsilon_{x,z} = 90\pi \text{ mm.mrad norm.}$ Middle : $\epsilon_{x,z} = 200\pi \text{ mm.mrad norm.}$ Right : full 6-D acceleration from 10 to 20 MeV.

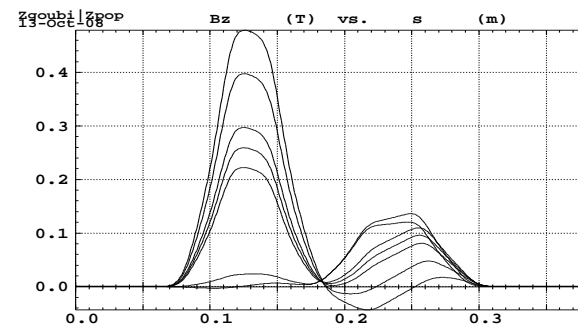
2.5.2 Closer to actual field shape : EMMA using ‘‘DIPOLES’’

It may be desirable to have a “theoretical” model of EMMA cell : for better understanding by moving parameters, for allowing use of ‘‘FIT’’, ...

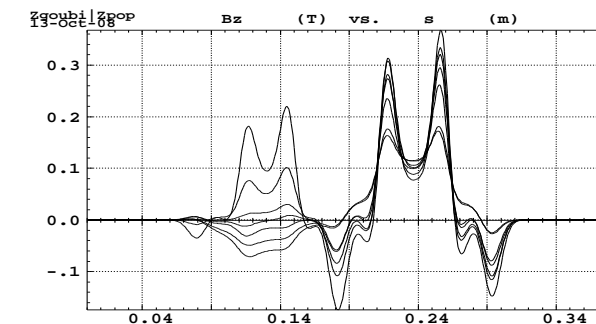
Here is what using ‘‘DIPOLES’’ may yield, including overlapping of fringe fields, “bell-shaped” type of longitudinal field distribution in QF and QD, one can play with it and try to reproduce the real EMMA cell (as was done with some success for KEK 150 MeV and for RACCAM) :



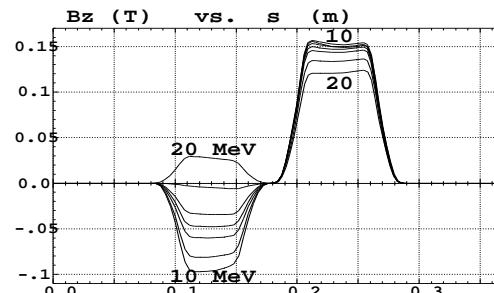
Field on closed orbits from 10 to 20 MeV



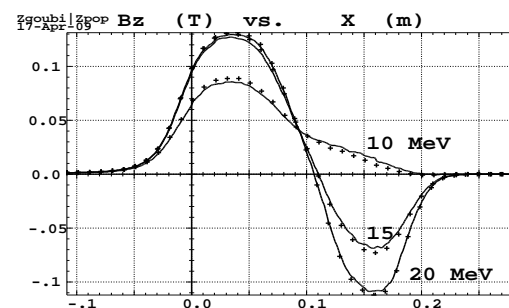
Field at maximum H stable amplitude, fixed energy, over a few turns



Field at maximum V stable amplitude, fixed energy, over a few turns



What it was earlier

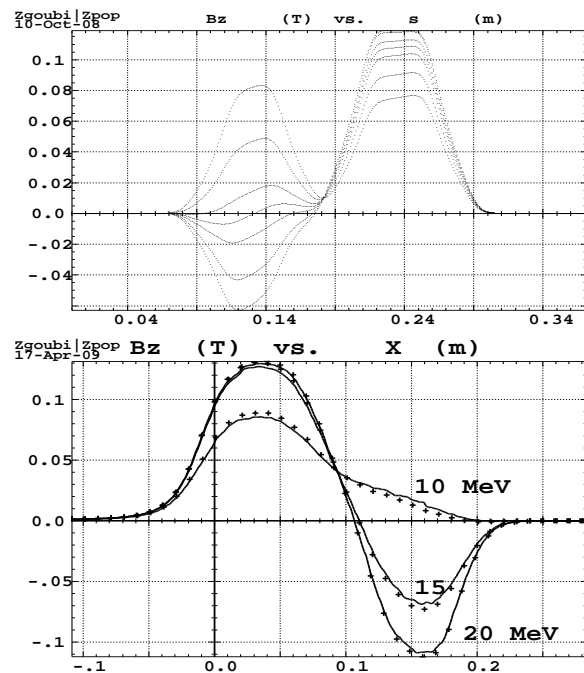


What TOSCA computations tell us it is...

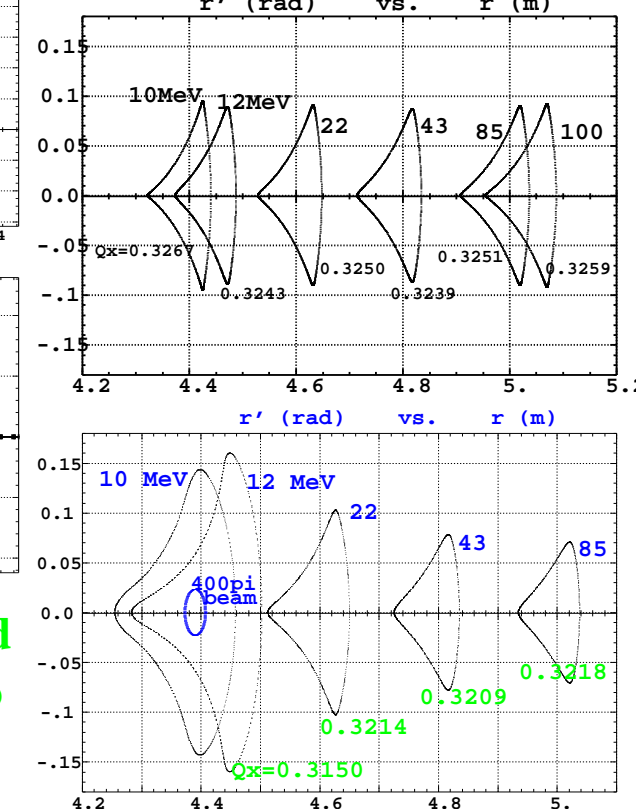
2.5.3 The idea, more precisely :

It may be desirable to have a “theoretical” model of EMMA cell : for better understanding by moving parameters, for allowing use of ‘‘FIT’’, ...

Try to reproduce the real EMMA cell (as was done with some success for KEK 150 MeV and for RACCAM) :

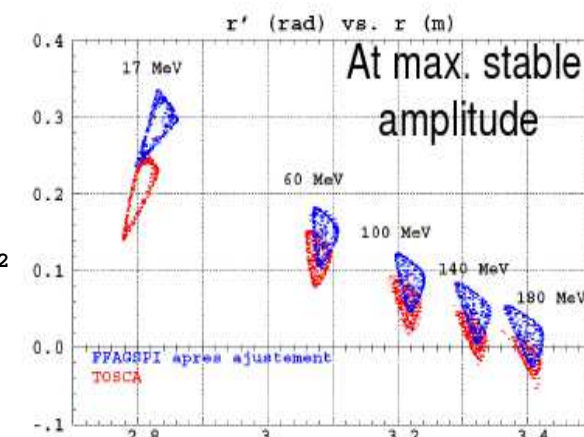


... reach the degree of reproduction achieved in the case of



By getting the field on closed orbits as close as possible to “reality” (TOSCA maps ? machine experiments ?) ...

KEK 150 MeV FFAG



RACCAM spiral FFAG

2.5.4 A new procedure for field maps, ‘‘EMMA’’

Details in Procs. PAC09 Vancouver.

There are three ways to use EMMA field maps :

(i) **a single field map, describing the FD cell with frozen quadrupole arrangement and fields.**

The “TOSCA” keyword does this job.

(ii) **the FD cell is described by a single pair of field maps,**

- of the “D” type (D/on, F/off)
- and of the type “F” (F/on, D/off)

The F-D transverse distance, d_{FD} , is frozen, field coefficients a_F, a_D are adjustable

(iii) **an ensemble of pairs of field maps in arbitrary number, each pair like in (ii) with its d_{FD} value attached.**

- Zgoubi will then interpolate in this set to get the field map corresponding to an arbitrary distance d_{FD} specified by the user.

- This working mode allows flexible use of the Zgoubi fitting procedure, with free and arbitrary variables a_F, a_D, d_{FD} .

(iv) **a unique “D”,“F” pair is used with arbitrary d_{FD} distance**

In all four cases, the cell length plays the role of the fourth variable in that EMMA cell, and is a free parameter liable to fitting.

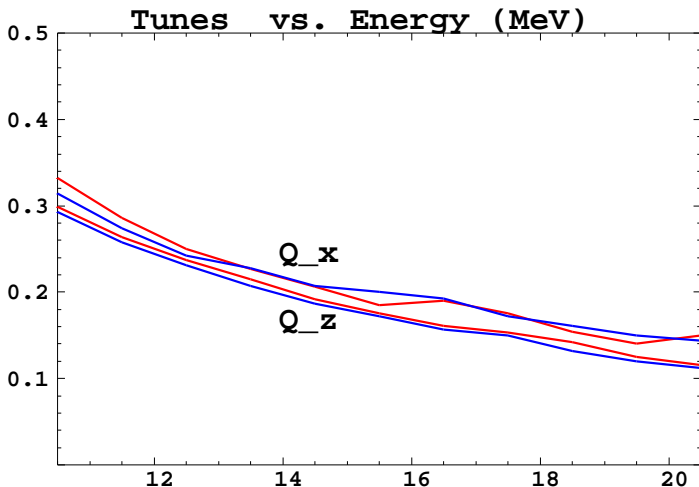


Figure 3: Tunes versus energy, case “D&F” ((i), blue, thick lines) and case “D+F” (red, thin lines).

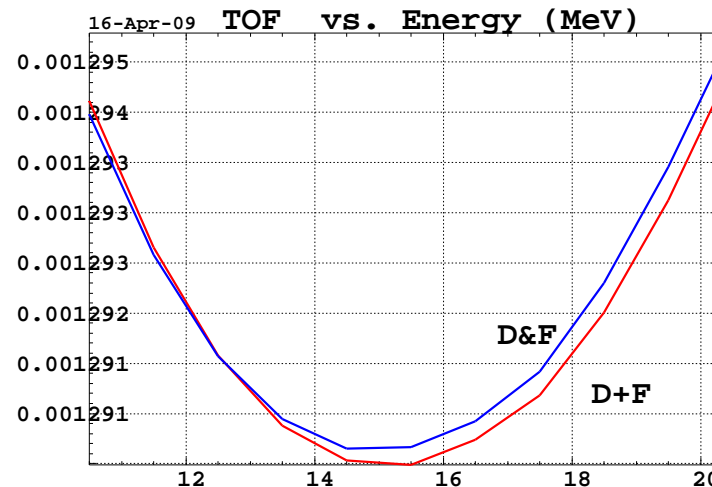


Figure 4: Time of flight parabola, “D&F” ((i), blue, thick line), “D+F” (red, thin line).

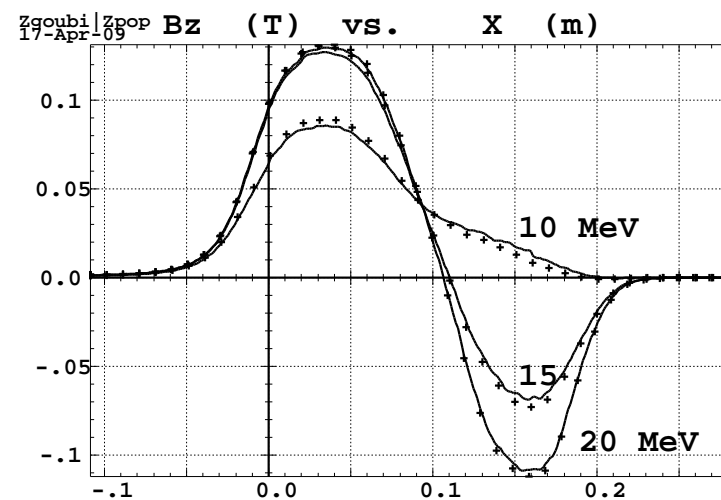


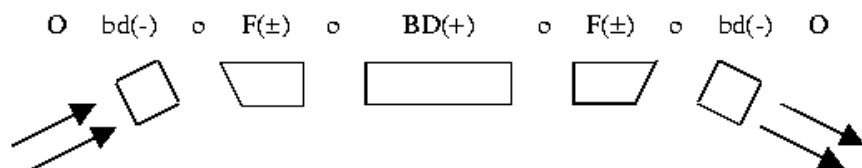
Figure 5: Field along closed orbits, case “D&F” (solid line) and case “D+F” (crosses). .

2.6 Pumplet-cell I-FFAG using "Dipoles", full acceleration cycle

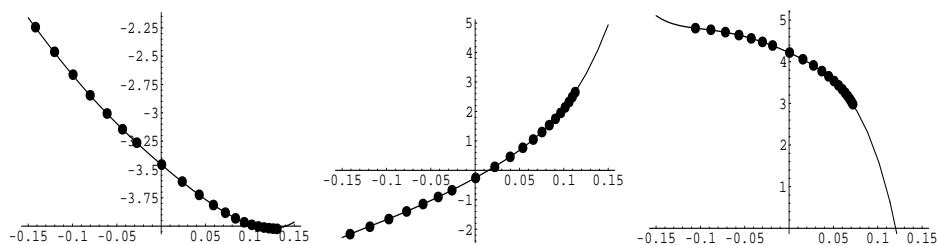
Electron model

Acceleration based on isochronous FFAG lattice
 Best use of the RF : on-crest acceleration
 (cyclotron-like)

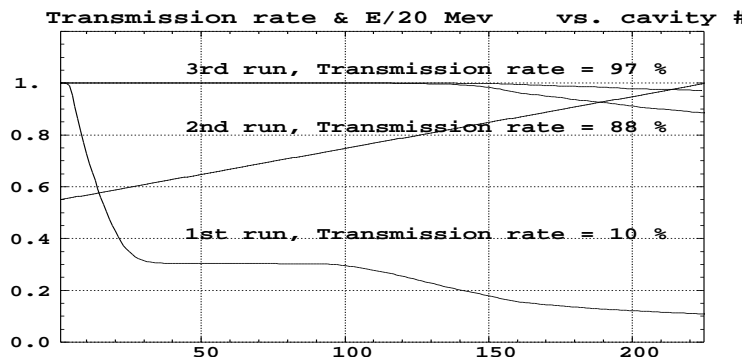
45 cells, 15 turns from 11 to 20 MeV, 40 kV/cell



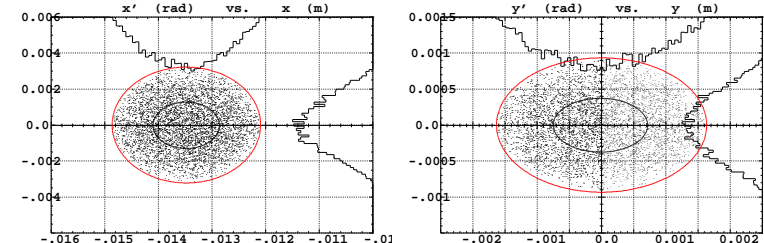
Difficulty for the integrator (the guy and the method) : tracking in highly non-linear fields (yet, comparable to scaling case)



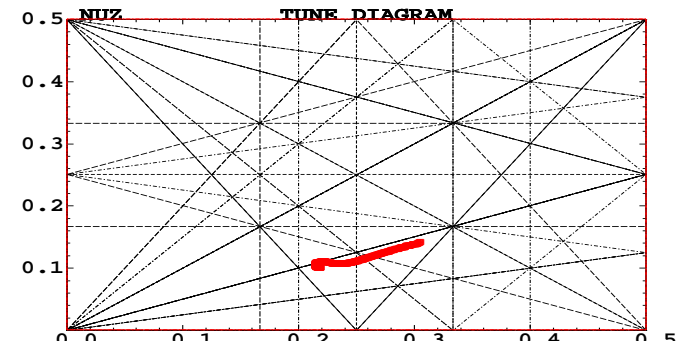
Iterative method



97% transmission for
 $\epsilon_{x/z} = 97/33 \pi \text{ mm.mrad normalized}$

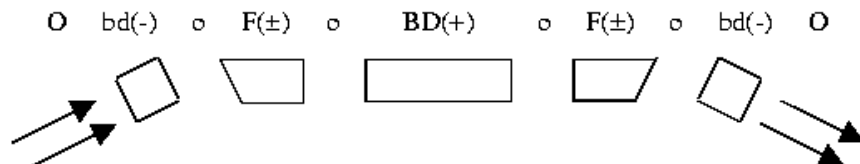


Beam path in tune diagram

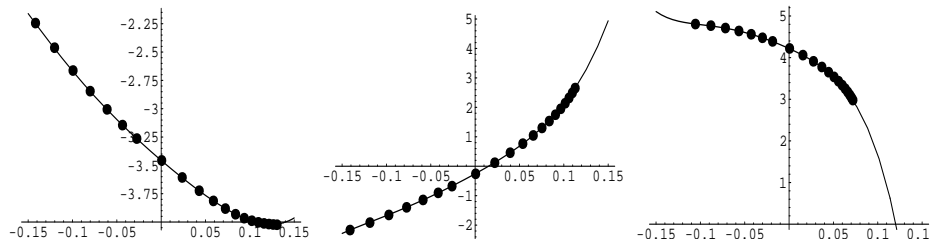


6-D transmission simulations in I-FFAG (cont') - Muon

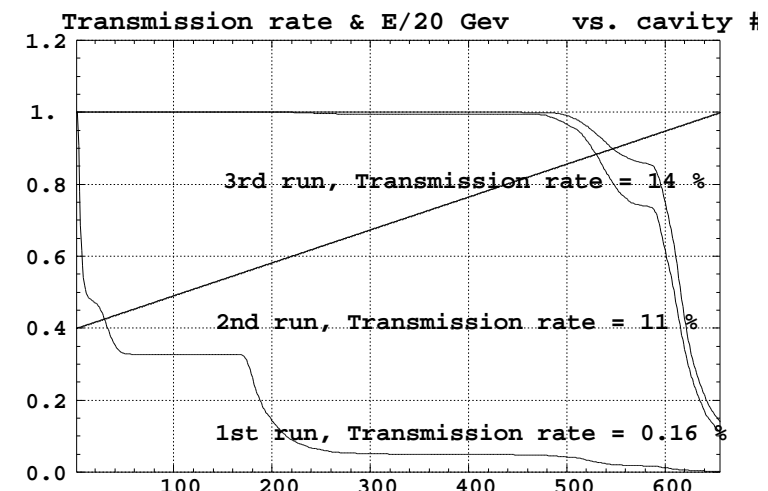
Acceleration based on isochronous FFAG lattice
 Best use of the RF : on-crest acceleration
 (cyclotron-like) using 200 MHz SCRF



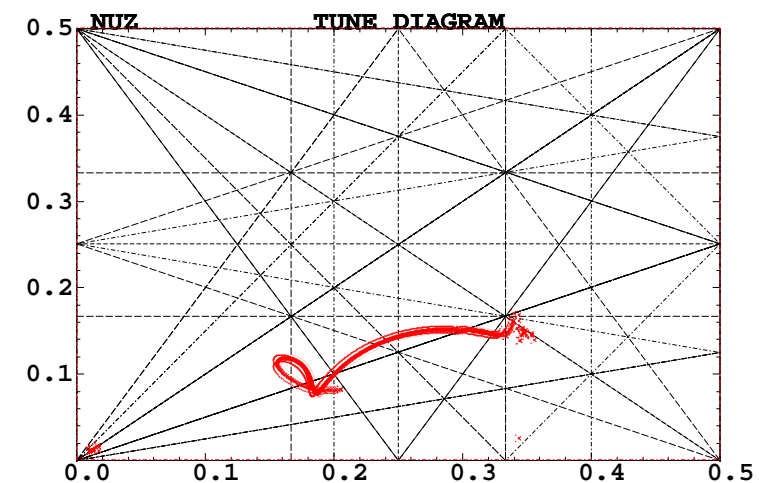
Difficulty for the integrator (the guy and the method) : tracking in highly non-linear fields (yet, comparable to scaling case)



Iterative method



Beam path in tune diagram



3 Synchrotron radiation

- Zgoubi allows the simulation of two types of synchrotron radiation (SR) effects
 - stochastic energy loss and ensuing perturbation on particle dynamics
 - radiated spectral-angular energy densities observed in the lab.

Energy loss and related dynamical effects

- The energy loss is calculated after each integration step Δs , in a classical manner, accounting for two random processes :
 - probability of emission of a photon
 - energy of the photon.
- Effects on the dynamic of the emitting particle :
 - alteration of the energy, or extended to
 - angular kick effect

Example - Emittance increase in the e^+e^- linear collider beam delivery system

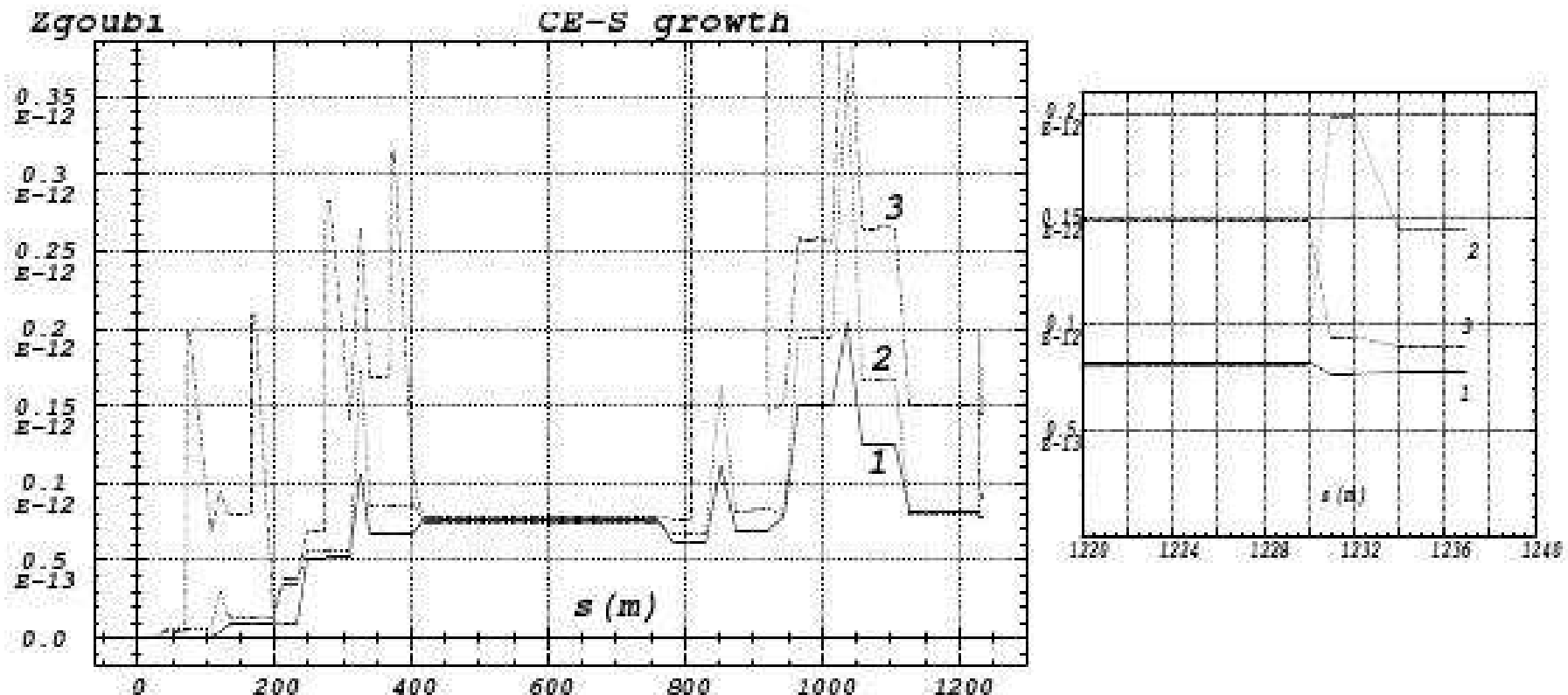
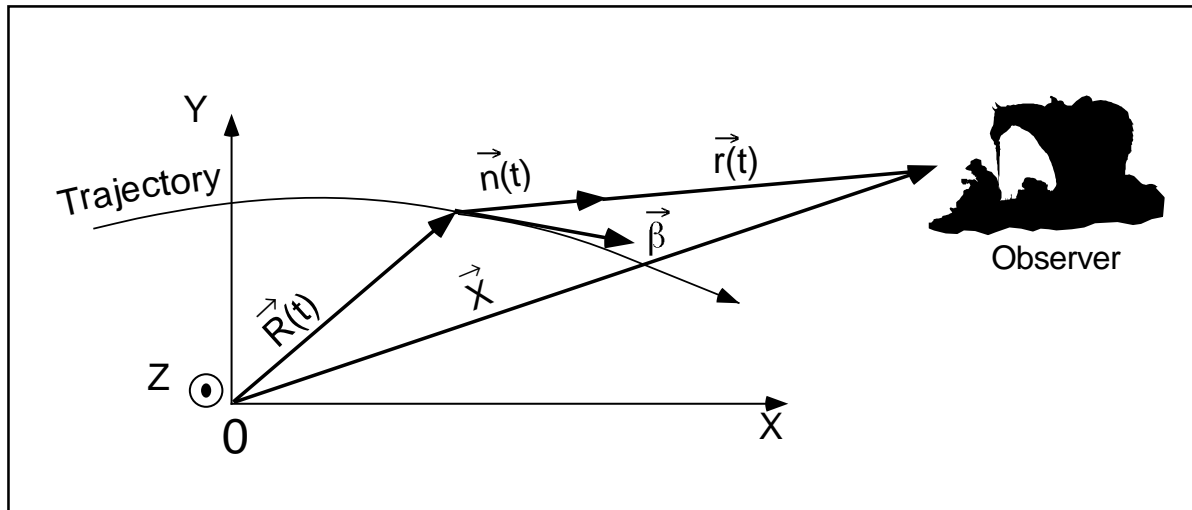


Figure 9: Horizontal CE-S variation ($S_x/\pi(s) - S_x/\pi(0)$) along TESLA-bds as obtained from the ray-tracing of $2 \cdot 10^4$ particles, in various cases of SR simulation (resp^{ly} 1, 2 and 3 in Table 1) :

- solid line : zero initial emittances, sextupoles off ;
- dashed line : initial emittances $\epsilon_{x0} = 10^{-11}$, $\epsilon_{z0} = 10^{-14}$ m.rad, sextupoles off ;
- dotted line : initial emittances $\epsilon_{x0} = 10^{-11}$, $\epsilon_{z0} = 10^{-14}$ m.rad, sextupoles are excited.

The last case shows a strong overshoot (cut out on the Figure) in the $s \approx 850$ m region due to chromatic distortions (see page 16) : this effect appears also in the low- β quad and FF region zoomed on the right plot (broken lines are due to particle coordinates being saved only at optical element ends).

Spectral-angular radiated densities



The ray-tracing ingredients provide the toolkit to compute

$$\vec{\mathcal{E}}(\vec{n}, \tau) = \frac{q}{4\pi\epsilon_0 c} \frac{\vec{n}(t) \times \left[(\vec{n}(t) - \vec{\beta}(t)) \times d\vec{\beta}/dt \right]}{r(t) \left(1 - \vec{n}(t) \cdot \vec{\beta}(t) \right)^3}, \quad \mathcal{B} = \vec{n} \times \vec{\mathcal{E}}/c$$

In the toolkit, amongst other tools :

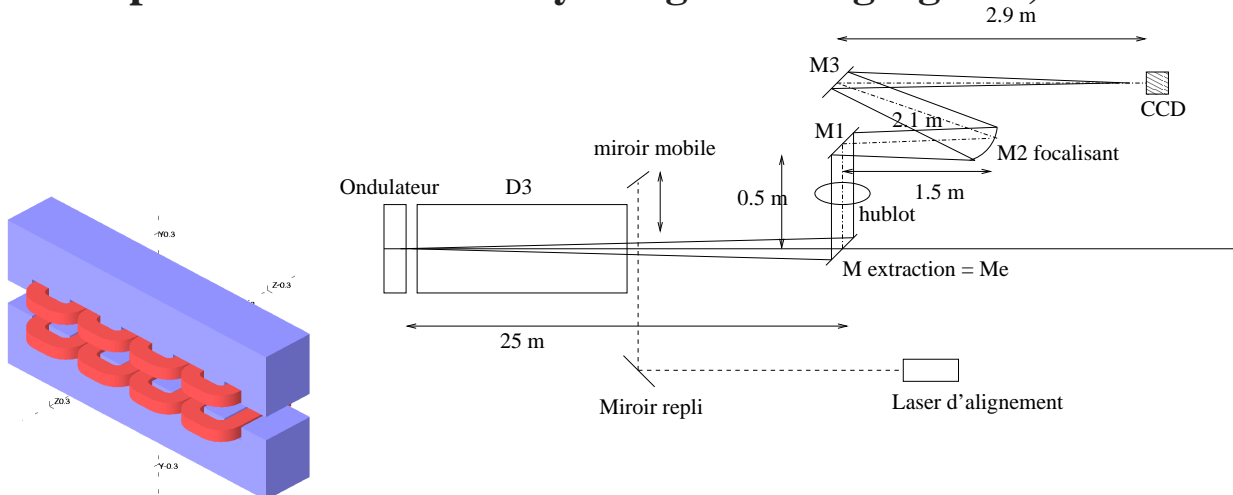
$$d\tau/dt = 1 - \vec{n}(t) \cdot \vec{\beta}(t)$$

$$d\vec{\beta}/dt = (q/m) \vec{\beta}(t) \times \vec{b}(t)$$

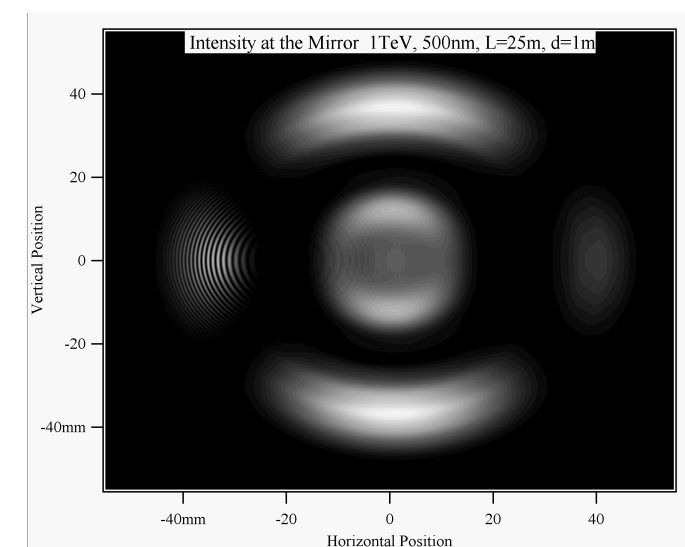
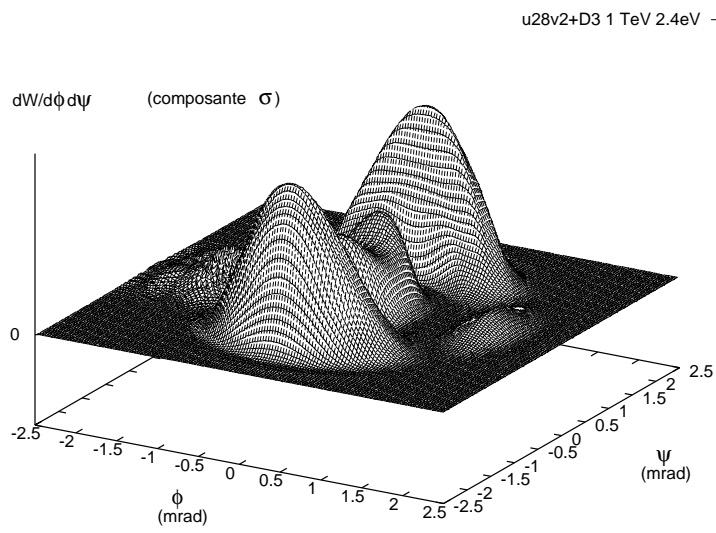
$$\vec{r}(t) = \vec{X} - R(t) \text{ and } \vec{n}(t) = \vec{r}(t)/|\vec{r}(t)|$$

EXAMPLE - Design of the SR beam diagnostics installations at LHC

This experience has been fully designed using Zgoubi, and then checked using SRW (ESRF).



LHC undulator upstream of a long dipole, and the optical system, drawn on that of LEP.



Intensity emitted (horizontal component) by 1 TeV protons, $\lambda = 500 \text{ nm}$, with a distance $d = 1 \text{ m}$ between the two sources, simulated with Zgoubi (left) and with SRW (right).

4 Spin

- The equation of spin precession

$$\frac{d\vec{S}}{dt} = \frac{q}{m} \vec{S} \times \vec{\Omega}, \quad \text{with} \quad \vec{\Omega} = (1 + \gamma G) \vec{b} + G(1 - \gamma) \vec{b}_{//}$$

Normalizing as earlier (remember : “ $u' = u \times \vec{B}$ ”) using $ds = vdt$, $\gamma mv = qB\rho$, $\omega = \Omega/B\rho$, etc., yields the form handled in the Fortran :

$$\boxed{\vec{S}' = \vec{S} \times \vec{\omega}}$$

- $\vec{S}(M_1)$ following a displacement Δs , is obtained from $\vec{S}(M_1)$ using truncated Taylor expansion

$$\vec{S}(M_1) \approx \vec{S}(M_0) + \frac{d\vec{S}}{ds}(M_0) \Delta s + \frac{d^2\vec{S}}{ds^2}(M_0) \frac{\Delta s^2}{2} + \frac{d^3\vec{S}}{ds^3}(M_0) \frac{\Delta s^3}{3!} + \frac{d^4\vec{S}}{ds^4}(M_0) \frac{\Delta s^4}{4!}$$

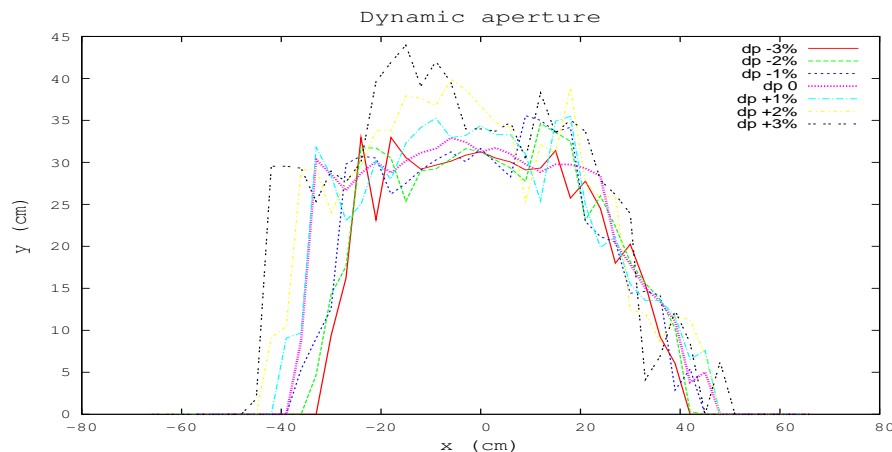
- Recurrent differentiation yields the $d^n\vec{S} / ds^n$ and $d^n\vec{B}_{//} / ds^n$ and at M_0 :

$$\vec{S}' = \vec{S} \times \vec{\omega}, \quad \vec{S}'' = \vec{S}' \times \vec{\omega} + \vec{S} \times \vec{\omega}', \quad \vec{S}''' = \vec{S}'' \times \vec{\omega} + 2\vec{S}' \times \vec{\omega}' + \vec{S} \times \vec{\omega}'', \quad \text{etc.}$$

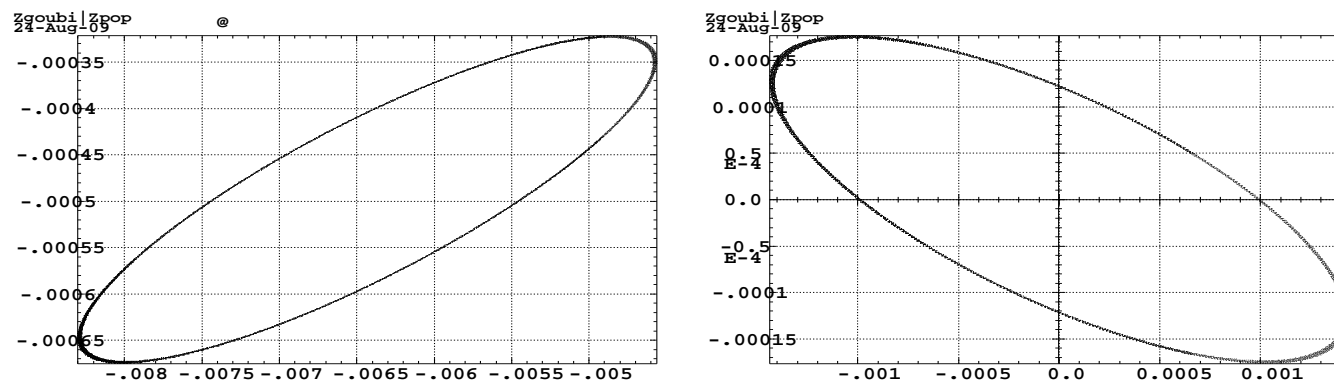
$$\vec{B}_{//} = (\vec{B} \cdot \vec{u}) \vec{u}, \quad \vec{B}'_{//} = (\vec{B}' \cdot \vec{u} + \vec{B} \cdot \vec{u}') \vec{u} + (\vec{B} \cdot \vec{u}) \vec{u}', \quad \text{etc.}$$

AGS

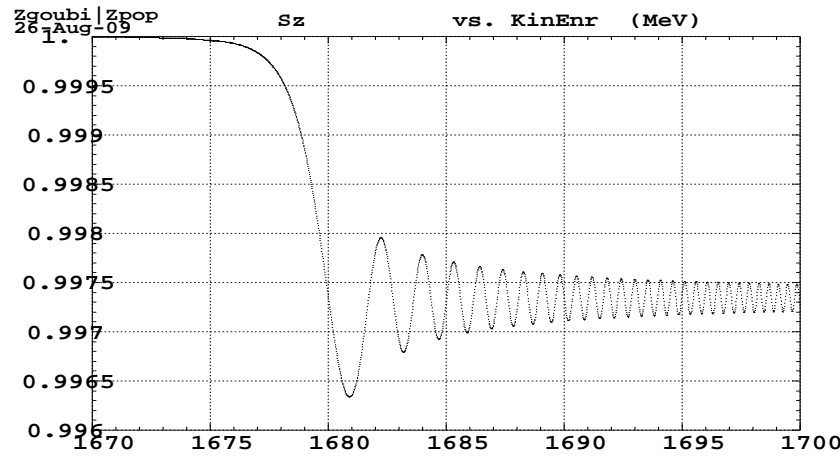
- AGS : 1010 elements in zgoubi.dat input, about half drifts / half magnets
- 240 main dipoles, straight axis, combined function, including sextupoles, simulated using ``MULTIPOL''



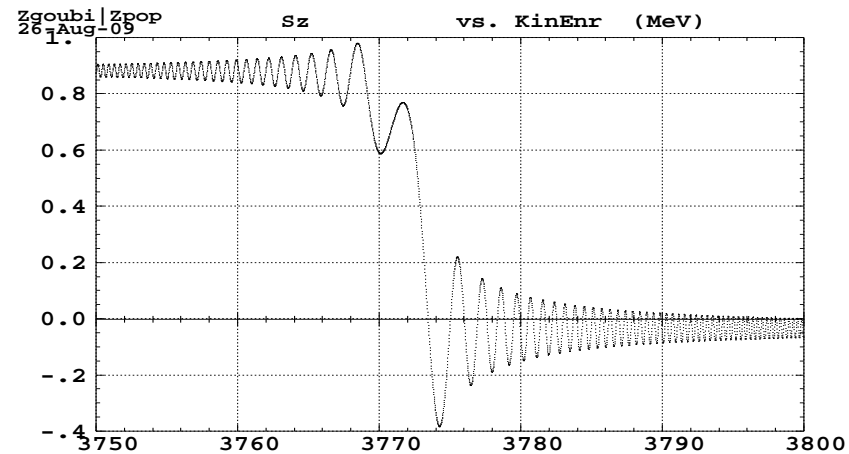
Left : DA in AGS, using automatic software calling Zgoubi.
Takes no more than minutes.



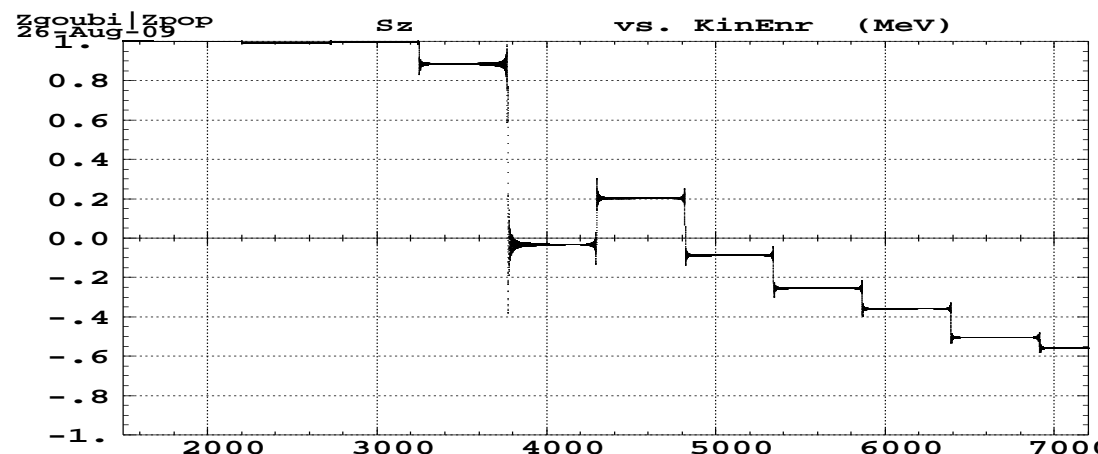
Right : 4×10^5 -turn in AGS, at fixed energy, xx' and yy'.



S_z versus kinetic energy. Crossing $\gamma G = 5$,
 $E = 1.678 \text{ GeV}$



Crossing $\gamma G = 9, E = 3.771 \text{ GeV}$ (right).



S_z versus kinetic energy. Full acceleration through imperfection resonances from $E = 1.5$ to
 7.2 GeV .

**THANK YOU
FOR
YOUR
ATTENTION**

